STDP Produces Robust Oscillatory Architectures That Exhibit Precise Collective Synchronization

David Bhowmik Murray Shanahan

[1]***Abstract*— It has been proposed that oscillating groups of neurons firing synchronously provide a mechanism that underlies many cognitive functions. In previous work, it has been demonstrated that, in a network of excitatory and inhibitory neurons, a synchronous response gradually emerges due to spike timing dependant plasticity (STDP) acting upon an external spatio-temporal stimulus that is repeatedly applied. This paper builds on these findings by addressing two questions relating to STDP and network dynamics in the context of pyramidal inter-neuronal gamma (PING) network architectures. Firstly, how does the choice of neuron model affect the learning of oscillation through STDP? Our experiments suggest that the earlier results hinge on the selection of a simple, biologically less realistic neuron model. Secondly, how do neural oscillators that have learned to oscillate only in response to a particular stimulus behave when connected to other such neural oscillators? We investigate this question in the context of a network of PING oscillators, in order to understand the relationship between coupling strength and the onset of synchrony, emulating the results of a classic experiment by Kuramoto.**

I. Introduction

THERE has been growing interest in brain dynamics and oscillatory behaviour within neuroscience communities due to the realization that different perceptual and behavioural states are associated with different brain rhythms. It has been hypothesized that disparate groups of neurons firing synchronously together provide a mechanism that underlies many cognitive functions, such as attention [1], associative learning [2], working memory [3], the formation of episodic memory [4,5], visual perception [6], and sensory selection [7]. Recently, a role for synchronization has been proposed in opening up communication channels between neuron groups[8], providing optimal conditions for information transfer[9]. Further to this, it has been suggested that transient periods of synchronization and desynchronization provide mechanism for dynamically forming coalitions of functionally related neural areas [10].

Spike Timing Dependent Plasticity (STDP) is a refinement of the Hebbian learning principle for spiking neural networks based upon the precise timing of pre-synaptic and post-synaptic spikes, and has been reported in many experimental studies [11]. STDP has further been studied in relation to oscillations. Levy *et al* [12] report that synaptic plasticity facilitates the formation of sub-assemblies within a network, each of which exhibits its own oscillatory dynamics, a phenomenon they refer to as *distributed synchrony*. Hosaka *et al* [13] demonstrate oscillatory dynamics in a network of excitatory and inhibitory neurons that has been trained using STDP with an external spatio-temporal stimulus that was repeatedly applied. In this latter work a synchronous response gradually emerges, and the synchrony becomes sharp as learning proceeds. The authors state that the generation of synchrony itself does not depend on the length of the cycle of external input, however they found that synchrony emerges once per cycle of the length of the external stimulus trained upon.

This paper addresses two issues relating to STDP and network dynamics. Firstly, how does the choice of neuron model affect the learning of oscillation through STDP? Secondly, how do neural oscillators that have learned to only oscillate in response to a particular stimulus behave when connected to other such neural oscillators?

In the first study, this paper assesses the effect that the neuron model has in a network of excitatory and inhibitory neurons that has been trained using STDP to respond by oscillating to a learnt stimulus. Neurons can be described by their bifurcation properties and the period of their super-critical limit cycle. For example, Type I neurons have a saddle node bifurcation and have a zero frequency super-critical limit cycle, where as Type II neurons can have a saddle node or an Andronov-Hopf bifurcation, but have a fixed frequency super-critical limit cycle[14]. For saddle node bifurcation neurons, the resting state of the neuron is at a sable equilibrium point. Incoming spikes are integrated and move the neuron voltage to a saddle point at which it enters a super-critical limit cycle and produces a spike. For Andronov-Hopf bifurcation neurons, there is a small sub-critical limit cycle around a stable fixed point. The position the neuron is at in this limit cycle will dictate the effect that incoming spikes have upon the limit cycle, and in turn the effect of future incoming spikes. The neuron dynamics can therefore resonate to the incoming signal. When the sub-critical limit cycle approaches a large amplitude spiking limit the neuron enters a super-critical limit cycle which elicits a spike. Both Type I and Type II spiking properties, as well as saddle node and Andronov-Hopf bifurcations are assessed in this paper.

The second question addressed in this paper concerns how neural oscillators that have learned to only respond to a particular stimulus would behave when connected to other such neural oscillators. Our previous work [15] explored the

David Bhowmik and Murray Shanahan are with the Department of Computing, Imperial College London, 180 Queen's Gate, London SW7 2AZ, UK.

relationship between simple (not neural) oscillator models and their neural counterparts by emulating neurally the Kuramoto critical coupling experiment[16]. This classic experiment showed that synchrony increases as connection strength is increased in a uniformly connected network of simple oscillators. Our previous work experimentally demonstrated that simple oscillator models display close behavioural similarities to networks of oscillating neural populations that are designed to produce an oscillatory response to any input. The work illustrated how neural models display greater spectral complexity during synchronization than the simple Kuramoto oscillator model, with several oscillatory frequencies coexisting within an individual neural oscillator population. It further demonstrated that at the point of maximum synchrony the neural systems not only display several coexisting frequencies within an individual oscillator population but that the system also shows deviations from a measure of full synchrony likely caused by these additional fluctuating influences. In this paper we revisit this experiment, but using instead neural oscillators that have been trained only to respond by oscillating to a learnt stimulus. We contrast the results to the synchrony in networks of neural oscillators in which the individual neural oscillators respond by oscillating to any input stimulus.

II. METHODS

A. Quadratic intergrate-and-fire neurons

The Quadratic Integrate and Fire (QIF) model [17] displays Type I neuron dynamics [18]. The time evolution of the neuron membrane potential is given by:

$$\frac{dV}{dt} = \frac{1}{\tau}(V - V_r)(V - V_t) + \frac{I}{C} \tag{1}$$

where V is the membrane potential, with V_r and V_t being the resting and threshold values respectively. C is the capacitance of the cell membrane. τ is the membrane time constant such that τ = RC with R being the resistance. I represents a depolarizing input current to the neuron.

An action potential occurs when V reaches a value V_{peak} at which point it is reset to value V_{reset}. The QIF model is equivalent to the theta neuron model described by Ermentrout and Kopell [19] if one sets the reset condition $V_{peak} = \infty$ and $V_{reset} = -\infty$. Like Börgers and Kopell [20] we use values $V_r = V_{reset} = 0$ and $V_t = V_{peak} = 1$, which reduces the above equation to:

$$\frac{dV}{dt} = aV(V - 1) + \frac{I}{C} \tag{2}$$

Here $a = \frac{1}{\tau}$ and is set to the value 2 for all experiments carried out in the paper. When working with the QIF model we assume a membrane potential between $V_r = -65$ mV and $V_t = -45$mV.

B. Izhikevich neurons

The Izhikevich (IZ) neuron model [21] is a two variable system that can model both Type I and Type II neurons depending upon how it is parameterized. The model simulates a refractory period, which is an advance on the QIF model when a Type I neuron is simulated. The time evolution of the model is defined as follows:

$$\frac{dV}{dt} = 0.04V^2 + 5v + 140 - U + I \tag{3}$$

$$\frac{dU}{dt} = a(bV - U) \tag{4}$$

$$\text{if V > 30, then}\{V \leftarrow c\ ,\ U \leftarrow U + d \tag{5}$$

$$\text{if U >15, then }\{U \leftarrow 15 \tag{6}$$

I is the input to the neuron. V and U are the voltage and recovery variable respectively, and a, b, c and d are dimensionless parameters. The values chosen for these are as follows: a=0.02, b=0.2, $c=-65+15\times r^2$, and $d = 8-6\times r^2$, where r is a value between 0 and 1 chosen from a uniform distribution. The chosen parameter values dictate that the Izhikevich neurons used in this paper are Type II neurons with a saddle node bifurcation. The extra term limiting U from going above 15 prevents over saturation of the recovery variable caused by high levels of input.

C. Hodgkin-Huxley neurons

The Hodgkin-Huxley (HH) model [22] is a Type II neuron with an Andronov-Hopf bifurcation, and is widely considered as the benchmark standard for neural models. It is based upon experiments on the giant axon of the squid. Hodgkin and Huxley found three different types of ion current: sodium (Na+), potassium (K+), and a leak current that consists mainly of chloride (Cl-) ions. Different voltage-dependent ion channels control the flow of ions through the cell membrane. From their experiments, Hodgkin and Huxley formulated the following equation defining the time evolution of the model:

$$C\frac{dV}{dt} = g_K n^4(V - E_K) - g_{Na}m^3h(V - E_{Na}) - g_L(u - E_L) \tag{7}$$

$$\frac{dn}{dt} = \alpha_n(V)(1 - n) - \beta_n(V)n \tag{8}$$

$$\frac{dm}{dt} = \alpha_m(V)(1 - m) - \beta_m(V)m \tag{9}$$

$$\frac{dh}{dt} = \alpha_h(V)(1 - h) - \beta_h(V)h \tag{10}$$

C is the capacitance and *n*, *m* and *h* describe the voltage dependence opening and closing dynamics of the ion channels. The maximum conductance of each channel are: g_k=120, g_{Na}=36 and g_L =0.3. The reversal potentials are set so that that E_k=-12, E_{Na}=115 and E_L=10.6. The standard rate

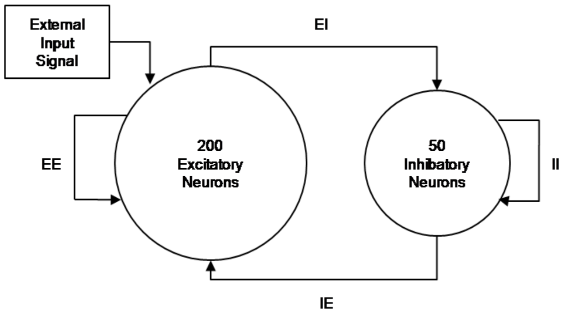

Fig. 1. Pyramidal inter-neuronal gamma (PING) architecture used for neural oscillatory nodes.

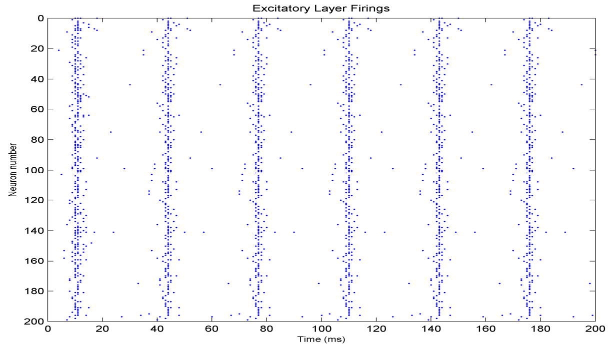

Fig. 2. Raster plot of neuron firings from the excitatory layer of a QIF PING node that has learnt to oscillate at 30 Hz.

functions for each channel are used and can be found in Hodgkin and Huxley's book [22].

All work in this paper using the HH model adjusts the neuron resting potential from 0 mV of the standard HH implementation to the more accepted value of 65 mV [23].

D. Synaptic model

A conductance synaptic model is used for experiments using the QIF and IZ models, which simply multiplies the incoming spike by a synaptic weight, whereas the HH model uses synaptic reversal potentials to further scale incoming spikes. The latter model is as follows:

$$I_j(t) = \sum_i w_{ij} t_i (Rev - V_j) \tag{11}$$

where $I_j(t)$ is the input to neuron j at time t, t_i is the spike from neuron i arriving at time t, and w_{ij} is the weight of the synapse connecting the two neurons. Rev is the reversal potential and V_j is the voltage of the target neuron. The reversal potentials for the model are set to the same values in all experiments. For excitatory inputs the reversal potential is set to 0 mV, and for inhibitory inputs the reversal potential is -70 mV. Not using a synaptic reversal model for the QIF and IZ models is equivalent to using a synaptic reversal model with reversal potentials set to +∞ mV for excitatory neurons and -∞ mV for inhibitory neurons.

E. Spike timing dependent plasticity

Spike timing dependant plasticity (STDP) is an empirically derived refinement of the Hebbian learning principal for spiking neural networks. STDP displays strengthening of correlated groups of synapses, the basic feature of Hebbian learning, as well as other desirable features such as firing-rate independence and stability [24].

Long-term plasticity depends on the exact timing relation, on the time scale of milliseconds, of the spikes from the pre-synaptic neuron and the spikes from the post-synaptic neuron. When the post-synaptic neuron fires at time t it initiates the synaptic weight update rule. The update rule considers pre-synaptic spike times (t-Δt) within a given window (τ). The update method used in this paper is an 'additive nearest neighbour' scheme, in which only the spike temporally nearest the time of the post-synaptic spike is considered, and the weight change is not dependent upon the current weight value. A pre-synaptic spike followed by a post-synaptic spike potentiates the synaptic weight, where as a post-synaptic spike followed by a pre-synaptic spike depresses the synaptic weight. The change in weight (Δw) is affected by the exponential of the time difference (Δt) and the learning rate constant (λ):

$$\Delta w = \lambda e^{\frac{-|\Delta t|}{\tau}} \tag{12}$$

For potentiation, the learning rate value λ is 0.3, and the window τ is 20 ms. For depression, the learning rate value λ is 0.3105 and the window τ is 10 ms.

F. Evolution of oscillatory nodes

Although groups of neurons firing together rhythmically can occur because of intrinsic firing patterns of excitatory principal cells or common input from a pacemaker, it is more common both in the cortex and the hippocampus that rhythmic firing happens as an emergent property of interactions between excitatory principal cells and inhibitory interneurons. Variations of this mechanism, known as pyramidal inter-neuronal gamma (PING), can give rise to both faster gamma oscillations, as well as slower oscillations such as theta in the cortex and the hippocampus [5].

Excitatory neurons drive the entire local network, including inhibitory interneurons. The most strongly driven inhibitory neurons will fire first and provide inhibition to numerous other inhibitory neurons. The inhibitory effect on all these neurons will disappear at approximately the same time. Affected inhibitory neurons will then fire roughly together, causing large numbers of inhibitory neurons to be entrained to a rhythm within just a few oscillatory cycles [25]. This rhythmically synchronized inhibition also affects the network's excitatory neurons with a fast and strong synaptic input [26] thus leaving only a short window for the excitatory neurons to fire after one period of inhibition wears off and before the next one starts [27].

Whilst the general PING architecture is well understood, the specific details required for both particular oscillatory frequencies and neuron model varies and involves a large space of parameter values within the general PING framework. In the present work, all neural populations used an excitatory layer of 200 neurons and an inhibitory layer of 50 neurons. The excitatory layer drives the entire network and so is the only one to receive external input. The networks were wired up with connections between excitatory neurons (EE), between inhibitory neurons (II), from excitatory to inhibitory neurons (EI) and from inhibitory to excitatory neurons (IE). The PING architecture used is illustrated in figure 1. In addition to the synaptic weight, a scaling factor of 7 was used on all synaptic current in the oscillatory populations for all neuron models to simulate networks of a larger size than we could feasibly simulate otherwise given the number of simulation runs in the experiments.

The parameters that were evolved were the length in milliseconds of the external stimulus presentation, the synaptic weights and delays, as well as the number of synaptic connections between source and target neurons in each pathway. The specific values for the weight and delay of each synaptic connection were generated using a normal distribution, with the means and variances for the weights and the delays being the parameters in the genome evolved. Weights were constrained to evolve values between 0 and 1 for excitatory connections and 0 and -1 for inhibitory connections. Long delays are quite unrealistic for a cluster of neurons in which all neurons are anatomically close together. In the cortex synaptic latency ranges from 0.2 ms to 6 ms [28]. In order to produce realistic results, excitatory delays were bounded between 1 ms and 10 ms. The IE and II delays were allowed to have a maximum value of 50 ms to simulate the effect of slow inhibitory interneurons, the behaviour of which was otherwise not modelled.

Two types of PING architecture networks were evolved. The first learnt a stimulus and then after learning would only oscillate to the learnt stimulus. The second did not use learning and so would oscillate to any input stimuli.

For the learning PING networks the input to the excitatory layer was generated from a Poisson process with parameter $\lambda = 0.3$. For QIF models the inputs were scaled by 45, for the IZ model they were scaled by 50, and for the HH models the inputs were scaled by 2.5 in order to provide sufficient stimulus to induce firing. Testing an individual consisted of three stages. The first stage trained the network. STDP was used only applied to the excitatory connections in the network. The amount of time trained for was also an evolved parameter in the learning evolutionary simulations, and STDP was stopped after this time. Next an individual was tested for 5000 ms of simulated time with the learnt stimulus to see how well it had learnt the stimulus. Finally an individual was tested for 5000 ms of simulated time with an alternative stimulus that it had not been trained for in order to see how it responds to other stimuli.

The evolutionary populations consisted of 20 individual genomes. After testing each individual was rated for fitness and probabilistically selected for the next generations parents based upon its fitness ranking. Crossover was performed on parent genomes after which mutation was applied to the offspring with a probability of 0.1.

The fitness function for the genetic algorithm consisted first of taking the spike firing times of the excitatory population and converting them to a continuous time-varying signal. This was achieved by binning the spikes over time, and then passing a Gaussian smoothing filter over the binned data. Next a Fourier transform was performed on the mean centred signal to produce the frequency spectrum of the signal. The first fitness term was applied to the firings from the simulation with the learnt stimulus after training. It was calculated by creating a scaled Gaussian centred around the desired frequency *f* in the spectrum of the form:

$$\text{clip} = 60\mathrm{G}\left(f, \frac{1}{2000} \right) \tag{13}$$

The frequency spectrum *s* was subtracted from this and normalized:

$$\text{fitness}_1 = \frac{-|clip - s|}{\sum clip} \tag{14}$$

An extra penalty was introduced to discourage frequencies outside the desired range. This was achieved by multiplying the frequency spectrum by -0.002 in the areas further away from the desired frequency whilst ignoring the area at and immediately around the desired frequency. The result was then normalized and added to fitness_1. The second fitness term was applied to the test in which the alternative stimulus was applied, and consisted of ensuring the amplitude of the peak frequency response for that test was below 0.5 so as to discourage firing to a non learnt stimuli. This was achieved by first locating the frequency with the highest amplitude A, and then calculating the second fitness term as follows:

$$\text{fitness}_2 = -\frac{20 - (\mathrm{A} - 0.5)}{20} \tag{15}$$

Both fitness terms were combined to give the overall fitness for an individual.

PING architectures that did not use learning were only evolved for the QIF model. Evolution consisted of one test in which a random stimulus was applied for 5000 ms of simulated time. The stimulus was generated using the Poisson process with parameter $\lambda = 0.4375$, and was scaled by 8 in order to induce sufficient firing. The fitness of an individual was calculated using only fitness_1 described above. Evolutionary selection, crossover and mutation were performed in the same way as with the evolution of the learnt PING architectures. Analysis of the resulting non-learning networks showed that the evolved oscillatory frequency (*f*) was mainly influenced by the EI/IE delay loop, for which EI mean delay + IE mean delay ≈ 1000/2*f*.

G. *Synchronisation metric*

The critical coupling experiment simulations in this work consisted of 64 neural oscillators connected together. Each neural oscillator consisted of an excitatory layer and an inhibitory layer. We only calculated synchrony for the excitatory neuron layers in the oscillators. The spikes of each neuron in each excitatory layer were binned over time, and

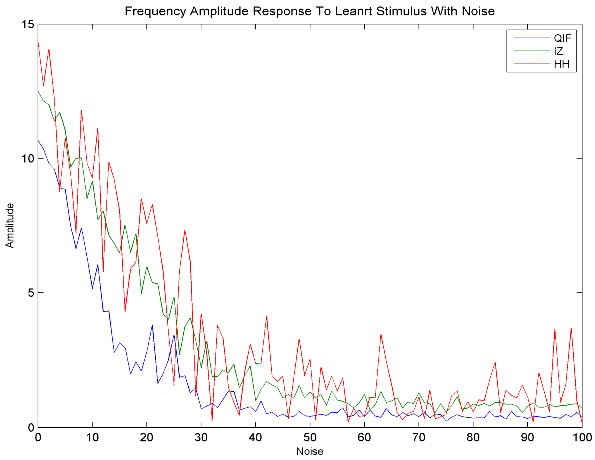

Fig. 3. Amplitude of desired 30 Hz frequency response for QIF, IZ and HH models with 0%-100% noise added to stimulus.

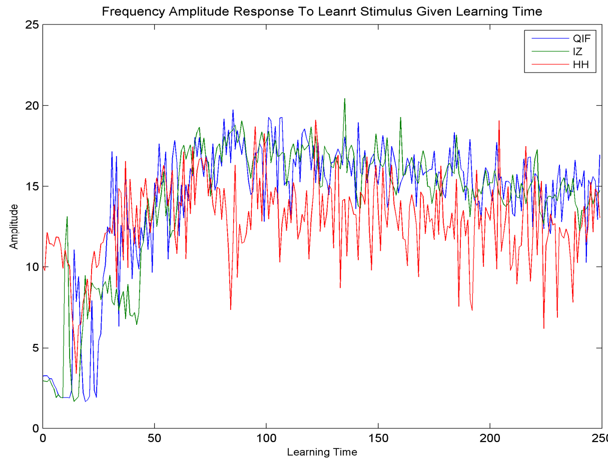

Fig. 4. Amplitude of desired 30 Hz frequency response for QIF, IZ and HH models after learning times from 1-250 ms.

then a Gaussian smoothing filter was passed over the binned data to produce a continuous time varying signal. Following this, we performed a Hilbert transform on the mean-centred filtered signal in order to identify its phase. The synchrony at time t was then calculated as follows:

$$\varphi = \frac{1}{t_{\max}} \sum_{t}^{t_{\max}} \left| \frac{1}{N} \sum_{j}^{N} e^{\theta_j(t) i} \right| \tag{16}$$

where $\theta_j(t)$ is the phase at time t of oscillatory population j. i is the square root of -1. N is the number of oscillators, and t_{max} is the length of time of the simulation.

III. Results

A. Neuron model and the learning of oscillation through STDP

Our first investigation explored how the neuron model affects the ability of a cluster of neurons to learn to oscillate. In order to explore this we evolved neural learning PING oscillators to oscillate at 30 Hz for QIF, IZ and HH neuron models. The evolutionary process is described in the methods section. It optimises the networks both for their ability to oscillate at the desired frequency in response to a learnt stimulus, as well as their ability to not respond to a non-learnt stimulus. Figure 2 shows a raster plot of the firings of the excitatory layer from the evolved QIF solution when it has been presented with a learnt stimulus after training. In accord with the finding of Hosaka *et al* [13], the network fires regularly at the stimulus presentation, and has narrow and pronounced periodic bands. These thin bands appear approximately every 33 milliseconds giving the 30 Hz oscillation desired.

Figure 3 shows how the networks respond to noise in the stimulus. The aim of this study is to ascertain if the network only responds by oscillating to the learnt stimulus and no other. To obtain this graph we took a trained network and the stimulus it was trained to and replaced a percentage of the stimulus with random data drawn from the same distribution. We then tested the network with the new stimulus for 5000 ms and measured the amplitude of the desired frequency response. We did this for every noise percentage from 0% to 100% and averaged the results over 10 sample runs. A 100% noise level represents a completely different pattern from the training stimulus, for which we expect the network not to respond at all. The QIF network performs the best, showing a gradual decline in the amplitude of the frequency response until it reaches a minimal response at 44% noise. Less than 0.5 amplitude implies that only a few neurons are firing hence no response is really being produced. With such a low noise to response threshold the QIF model is the most highly selective to only its learnt stimulus. The IZ model performs almost as well. The HH model performs poorest with a less pronounced frequency amplitude decline as noise rises, and also a less stable response throughout. The less stable response is due to a high variance in the amplitude over the 10 sample runs, either meaning that the network is very sensitive to particular afferents which may or may not appear in any of the 1000 runs performed and their particular noise level and sample run, or that the network is just inherently more volatile.

We next explored the effect that learning time has upon the networks. For each network type we took a stimulus and trained the network on it for a given time t. We then tested the network on the stimulus for 5000 ms and measured the desired frequency amplitude response. We did this for every learning time t between 1 ms and 250 ms. We averaged the results over 10 sample runs. Figure 4 shows the results. Some unpredictability can be seen below 20 ms learning time that may be expected for a 33 ms stimulus. After this the amplitude rises steadily until it stabilises around 100 ms. Beyond this there is some dip with not much variation. The learning time is very quick and only three stimulus presentations are required to learn maximally. The HH model performs poorest with a less stable response throughout due to a high variance in the amplitude over the 10 sample runs, as well as an overall lower amplitude. Variance of amplitude in this case is not due to particular afferents being present on particular runs as all are present

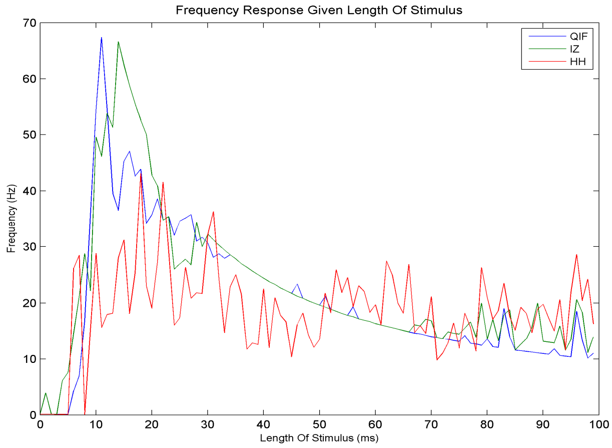

Fig. 5. Frequency response for QIF, IZ and HH models after learning with varying stimulus lengths.

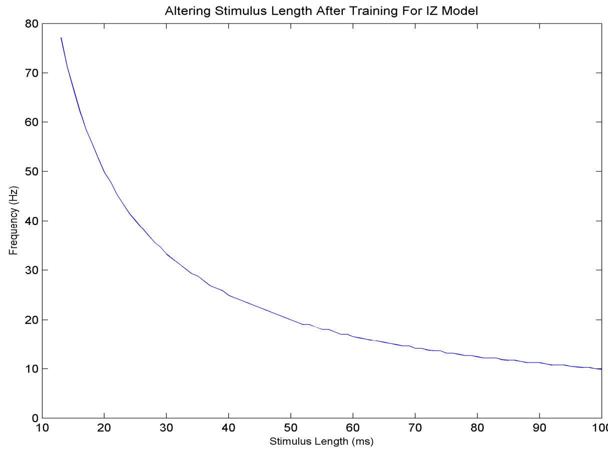

Fig. 6. IZ model after learning with 14 ms stimulus. Frequency response for varying stimulus lengths presented after learning .

on all runs, and so is due to the network being more volatile. This suggests that the variance in amplitude in the noise experiments is also due to volatility.

Figure 5 shows the effect of changing the length in milliseconds of the stimulus. To achieve this we took a stimulus of length *t*, trained the network on it, and then tested the network for 5000 ms on the same stimulus. We did this for every stimulus length *t* between 1 ms and 100 ms, and averaged the results over 10 sample runs. All learning stages for all stimulus lengths *t* had the same learning time. We located the frequency with the highest amplitude only. From the figure we can see that none of the models respond significantly to stimuli less than 10 ms long. Beyond this, the figure shows that for both QIF and IZ models, the length of the stimulus is roughly proportional to the frequency (*f*), with f=1000/t. This cannot be said of the HH model which is unable to use the same network architecture to learn to oscillate at different frequencies, given only a change in the stimulus length. Having found a dependency on stimulus length, we removed the inhibitory layer from the networks and found it made no difference to the performance of QIF, IZ and HH models. We conclude that, regular repetition of a stimulus to a network that has been trained using STDP will cause oscillation at the frequency of presentation. For the HH model this further means that whilst stimulus length is important in achieving the result, the tuning of other variables is necessary to achieve the desired oscillation.

The fact that oscillatory frequency is dependent upon the length of the presentation can be elucidated by the work of Masquelier *et al*[30]. They report that during learning with STDP, uncorrelated firings are depressed, whilst the synaptic connections with the afferents that took part in the firing of a neuron are potentiated. Further to this, '*Each time the neuron discharges in the pattern, it reinforces the connections with the presynaptic neurons that fired slightly before in the pattern. As a result next time the pattern is presented the neuron is not only more likely to discharge to it, but it will also tend to discharge earlier'*[14]. The fact that neurons learn to always respond to a particular stimulus implies that the regular repetition of a stimulus would cause the network to fire regularly at the stimulus presentation, and that this firing would become earlier and sharper, in the sense of producing narrower and more pronounced periodic bands, as learning proceeds. Hence, the resulting synchrony.

It follows from this that after an appropriate period of learning the frequency of the oscillation can be adjusted by simply altering the length of the stimulus, as it is only the beginning of the stimulus that is required to induce firing. To test this hypothesis we generated a stimulus of 100 ms, but only trained the network on the first 14 ms repeatedly until a satisfactory amplitude response was attained. We then tested the network for 5000 ms with the stimulus but only using the first *t* milliseconds repeatedly. We did this for every value of *t* between 13 and 100 ms. As can be seen by the results for the IZ model shown in figure 6, the hypothesis is correct. Hosaka *et al* [13] state that in a network of excitatory and inhibitory neurons, STDP transforms a spatiotemporal pattern to a temporal pattern. However, from the evidence above we conclude that the resultant temporality is not due to the network dynamics that result from the PING architecture, but is an artifact of repeated *periodic presentation* of a learnt stimulus. The network will respond "synchronously" whenever the stimulus is presented.

Given that the frequency of the oscillations in the evolved networks that did not use learning were caused by the EI/IE delay loop, we can conclude that repeated post-learning presentation of the stimulus overrides or interferes with the oscillatons that would otherwise be caused by the delays in the PING architecture. A fast EI/IE loop will feed back and subside before the next learnt stimulus response. In this case oscillations from the periodic stimulus will take precedence over PING oscillations. Using neurons of either Type I or Type II classification produces equivalent results with STDP. However, the HH model does not perform in the same manner. The difference in the HH model is the Andronov-Hopf bifurcation and the neuron's synaptic reversal potential. The result is a less robust network that is also unable to use the same architecture to learn to respond to stimuli that have a variety of presentation times.

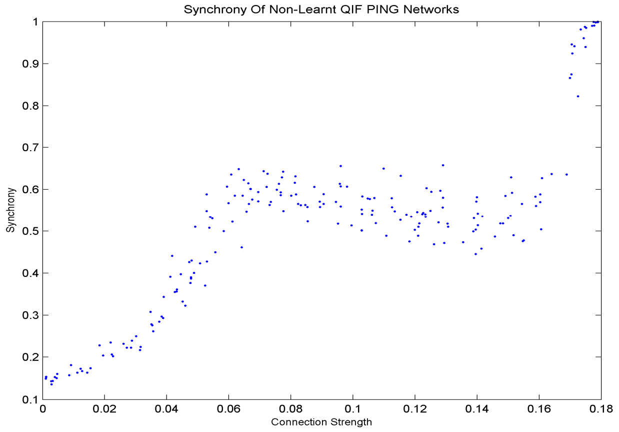

Fig. 7. Synchrony of QIF models that have not used STDP to train to respond to a particular stimulus and therefore responds to any stimuli.

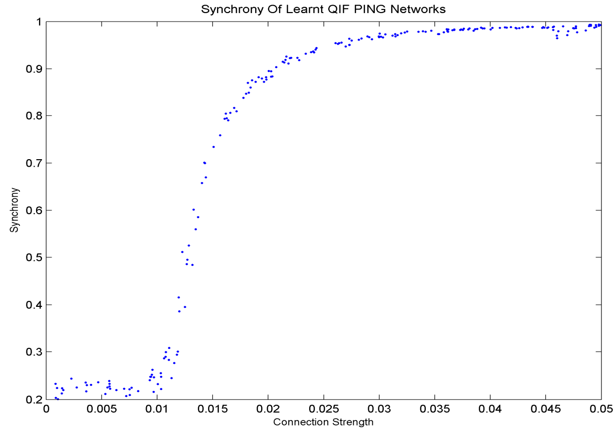

Fig. 8. Synchrony of QIF models that have used STDP to train to respond only to a particular.

B. *Kuramoto experiment*

Our next investigation explored the critical coupling experiment[16] in which synchrony increase smoothly but rapidly as connection strength increases in a uniformally connected network of oscillators. In this experiment we use PING neural oscillator nodes that had learnt to oscillate at different frequencies.

Given the findings of the previous investigation, we were able to generate every frequency of oscillation between 10 Hz and 50 Hz for QIF neurons, by training our evolved solution and varying the stimulus length and the learning time. Whilst our findings in the previous section showed that the inhibitory layer is not essential for producing the oscillation in these learning networks, we retained the inhibitory PING architecture to reduce the possibility of neuron saturation (by which we mean all neurons firing all the time) when connecting many oscillators together.

In order to compare the results to neural oscillators that had not learnt, we evolved every frequency of oscillation between 10 Hz and 50 Hz for QIF neurons but without using learning, and so relying on the evolved delays to produce to oscillation [15]. The evolution of these types of networks is described in the methods.

For simplicity, Kuramoto assumed that the distribution of oscillator intrinsic frequencies was unimodal and symmetric about its mean frequency, as in a Gaussian distribution for example [31]. We have evolved PING architectures for every frequency between 10 Hz and 50 Hz. In line with Kuramoto's specification we selected from these oscillators using a Gaussian distribution with a mean of 30 Hz. The variance we chose in order to ensure a good spread of different oscillator frequencies was 10 Hz.

In all our experiments we used 64 neural oscillator nodes to form a network. Given a learnt PING node, external input to the excitatory layer along with the learnt EE connections induces the intrinsic oscillation at the frequency the node was generated for. For a non-learnt PING node, external input to the excitatory layer along with the PING architecture induces the intrinsic oscillation at the frequency the node was generated for. The phase of each oscillator was determined by the time at which external input to the oscillator was started, which varied from 0 ms to 100 ms. The slowest oscillator was 10 Hz and therefore a random start point ranging from 0 ms to 100 ms allowed for 10 Hz oscillators (as well as all oscillators of higher frequency) to be completely out of phase with each other. The neurons in the excitatory layers of each node were synaptically connected to the neurons in the excitatory layers of each other node with a connection ratio of 0.2. The experiments involved a sweep of 200 synaptic weights for all inter-node connections. Weights were set to the same value within each iteration in the parameter sweep, but with each different iteration having a different synaptic weight. On each sweep the overall synchrony of the network was measured. The networks were simulated for 2000 ms for each iteration of the sweep. Each network comprised 16000 neurons and 36,256,000 synapses.

Beyond a particular high coupling value, the network models exhibited "saturation", meaning that all excitatory neurons in all nodes were firing continuously. The results shown here display data up to the respective point of saturation for each model type as data beyond this point is not noteworthy.

Figure 7 shows the synchrony results for the evolved PING architectures that **do not use learning**. At 0 connection strength there is a synchrony of around 0.2, which indicates no synchrony at all except for coincidental alignments in phase. Synchrony rises with connection strength but so too does the spread of the dots, indicating some variation in behaviour with these systems. The synchrony levels off at 0.07 connection strength and remains the same until there is a major discontinuity at 0.17 connection strength.

By contrast figure 8 show the synchrony for the neural oscillators **that had learnt to oscillate**. Within a critical region of connection strengths, synchrony can be seen to increase smoothly but rapidly as connection strength increases, in accord with Kuramoto's findings. The connection strength is effective at different levels to the non-learning PING model due to different sensitivities in the evolved solutions, Poisson process parameters, and scaling factors. However the behaviour is the key difference to note. There is a very tight sinusoidal increase, indicating little variation in behaviour with these learnt systems, unlike those in figure 7. There are also no discontinuities. The systems that have been pre-trained using STDP produce well defined and precise collective behaviour, unlike those not trained.

IV. Discussion

It has been shown that STDP generates robust synchronous responses. After learning, the networks are highly selective for their learnt stimulus and do not respond to other stimuli. Effective learning is possible within only three stimulus presentations. Given that the resultant oscillatory frequency is dependent upon the length of the presentation, the hypothesis that the frequency of the neural oscillator can be adjusted by simply altering the length of the stimulus was experimentally proven. Further to this, the critical coupling experiment demonstrates that the collective behaviour of oscillatory architectures that have been pre-trained using STDP is well defined and precise, in contrast to those that have not been trained.

Type I and Type II neuron classification does not make any difference in learning to respond to the temporality of stimuli, nor to the robustness thereof. However, the HH model, which uses an Andronov-Hopf bifurcation and neuronal synaptic reversal potential, does not perform robustly, and requires specific tuning of parameters to achieve desired oscillatory frequencies. It is interesting to note that the more biologically realistic model is less robust and requires specific parameter turning, leaving open the question of how the brain facilitates this in order to achieve a broad variety of oscillatory frequencies in response to different stimuli. Given these findings it might be concluded that simpler more robust neural models are more appropriate for use in a neural engineering context.

References

[1] Jensen O,. Kaiser J,. Lachaux J. (2007). Human gamma-frequency oscillations associated with attention and memory. Trends in Neurosciences, 30(7), 317–324.W.-K. Chen, *Linear Networks and Systems* (Book style). Belmont, CA: Wadsworth, 1993, pp. 123–135.

[2] Miltner W.H.R., Braun C., Matthias A., Witte H,.Taub E.(1999). Coherence of gamma-band EEG activity as a basis for associative learning. Nature, 397(6718), 434–436.

[3] Siegel M., Warden M.R., Miller E.K. (2009). Phase-dependent neuronal coding of objects in short-term memory. Proceedings of the National Academy of Sciences of the United States of America, 106(50), 21341-6.

[4] Lisman J. (2005). The theta/gamma discrete phase code occuring during the hippocampal phase precession may be a more general brain coding scheme. Hippocampus. 2005;15(7):913-22.

[5] Nyhus E., and Curran T. (2010). Functional role of gamma and theta oscillations in episodic memory. Neuroscience and biobehavioral reviews. 2010;34(7):1023-35.

[6] Fries, P., Reynolds, J. H., Rorie, A. E., and Desimone, R. (2001). Modulation of oscillatory neuronal synchronization by selective visual attention. Science, 291(5508):1560–1563. 2.1.

[7] Fries, P., Schroder, J., Roelfsema, P. R., Singer, W., and Engel, A. K. (2002). Oscillatory neuronal synchronization in primary visual cortex as a correlate of stimulus selection. Journal of Neuroscience, 22(9):3739–3754.

[8] Fries P. (2005). A mechanism for cognitive dynamics: neuronal communication through neuronal coherence. Trends in cognitive sciences. 2005;9(10):474-80.

[9] Buehlmann, A., & Deco, G. (2010). Optimal Information Transfer in the Cortex through Synchronization. (K. J. Friston, Ed.)PLoS Computational Biology, 6(9).

[10] Shanahan M. (2010). Metastable chimera states in community structured oscillator networks. Chaos, 20(1), 013108.

[11] Abbott, L. F., & Nelson, S. B. (2000). Synaptic plasticity: taming the beast. Nature neuroscience, 3 Suppl(november), 1178-83.

[12] Levy, N., Horn, D., Meilijson, I., & Ruppin, E. (2001). Distributed synchrony in a cell assembly of spiking neurons. Neural Networks, 14(6-7), 815-24.

[13] Hosaka, R., Ikegnuci, T., Nakamura, H., Akaki, O. (2004). Information Transformation from a Spatiotemporal Pattern to Synchrony through STDP Network. Procs IJCNN 2004, 1475-1480.

[14] Izhikevich, E. (2007). Dynamical Systems In Neuroscience. Cambridge University Press, 2007.

[15] Bhowmik D., Shanahan M. (2012). How Well Do Oscillator Models Capture the Behaviour of Biological Neurons? Proc IJCNN 2012, 1-8.

[16] Kuramoto, Y. (1984). Chemical Oscillations, Waves and Turbulence. Springer-Verlag, Berlin, 1984.

[17] Latham, P.E., Richmond, B.J., Nelson, P.G., Nirenberg, S. (2000). “Intrinsic dynamics in neuronal networks. i. theory.” Journal of Neurophysiology 83(2), 808–827.

[18] Ermentrout, B. (1996). Type I membranes, phase resetting curves, and synchrony. Neural Computation 8(5), 979–1001.

[19] Ermentrout, G.B., Kopell, M.(1986). Parabolic bursting in an excitable system coupled with a slow oscillation. SIAM Journal on Applied Mathematics 46(2), 233.

[20] Börgers, C., and Kopell, N. (2005). Effects of noisy drive on rhythms in networks of excitatory and inhibitory neurons. Neural Computation 17(3), 557–608.

[21] Izhikevich, E. M. (2003). Simple model of spiking neurons. IEEE transactions on neural networks. 14(6), 1569-72.

[22] Hodgkin, A.L., Huxley, A.F. (1952). A quantitative description of ion currents and its applications to conduction and excitation in nerve membranes. J. Physiol. (Lond.), 117:500-544.

[23] Gerstner, W., Kistler, W. (2002) Spiking neuron models. Cambridge University Press, 2002.

[24] Song, S., Miller, K.D., Abbott, L.F (2000). Competitive Hebbian learning through spike-timing-dependent synaptic plasticity. Nature neuroscience. 2000;3(9):919-26.

[25] Vida, I., Bartos, M., Jonas, P. (2006). Shunting inhibition improves robustness of gamma oscillations in hippocampal interneuron networks by homogenizing firing rates. Neuron, 49(1), 107-17.

[26] Papp, E., Leinekugel, X., Henze, D.A., Lee, J., Buzsáki, G. (2001). The apical shaft of CA1 pyramidal cells is under GABAergic interneuronal control. Neuroscience 102(4).

[27] Hasenstaub, A., Shu, Y., Haider, B. (2005). Inhibitory postsynaptic potentials carry synchronized frequency information in active cortical networks. Neuron. 2005;47(3):423-35.

[28] Markram, H., Lübke, J., Frotscher, M., Roth, A., Sakmann, B. (1997). Physiology and anatomy of synaptic connections between thick tufted pyramidal neurones in the developing rat neocortex. The Journal of physiology. 1997;500 (Pt 2):409-40.

[29] Fidjeland, A.K., Shanahan, M. (2010). Accelerated Simulation of Spiking Neural Networks Using GPUs. Proceedings IJCNN 2010.

[30] Masquelier, T., Guyonneau, R., & Thorpe, S. J. (2008). Spike timing dependent plasticity finds the start of repeating patterns in continuous spike trains. PloS one, 3(1), e1377.

[31] Strogatz, S. (2000). From Kuramoto to Crawford: exploring the onset of synchronization in populations of coupled oscillators. Physica D: Nonlinear Phenomena, 143(1-4), 1-20.